Intro to Non-Hermitian QM

Lisa Lin

March 25, 2020

1 Introduction

We love Hermitian operators. Physics loves Hermitian operators. After all, Hermitian operators have real spectra, which means they are observables!

But, as it turns out, we can extend the title of "observable systems" to a much broader category of Hamiltonians invariant under parity ($\mathcal{P}$) and time reversal ($\mathcal{T}$) operators (we will explore why this is the case in the following section!). The concept of replacing the Hermitian condition of self-adjointness with the weaker condition of $\mathcal{PT}$ invariance to obtain new classes of Hamiltonians with real, positive spectra, was pioneered by [2]. This extension of conventional quantum mechanics was initially regarded as a mathematical curiosity [1], but has since become a focus of applications in a wealth of fields, including solid state physics [6], population biology [14], neutrino physics [15], and fluid dynamics [16].

An implication of this non-Hermiticity is that such systems are also *nonconservative*. It is important to stress that, while *locally* there can be energy gain and loss, the energy of the *global* system is conserved, and so the sanctity of high school physics classes everywhere remains intact. We can obtain non-Hermitian systems by looking at these local systems in isolation. For instance, a lightbulb converts electrical power into radiation, which is an energy loss from the perspective of the circuit. And in particle decays, if we ignore the energy going to decay products, the local system of the particle itself experiences energy loss. On the other hand, a laser passing through an amplifying medium *gains* energy.

In such "open" systems described by effective non-Hermitian Hamiltonians, there often appear points in parameter space, called "exceptional points" (EPs), at which both eigenvalues *and* eigenvectors of an operator become degenerate. Many of the strange and fascinating aspects of these gain/loss systems focus around exceptional points.

In this paper, we will primarily focus our discussion on PT symmetry, exceptional points, and their applications in optics and photonics.

2 PT Symmetry

2.1 Properties and Definitions

The parity operator $\mathcal{P}$ flips the sign of spatial coordinates:

$$\mathcal{P} : \vec{r} \to -\vec{r}$$

while the time operator $\mathcal{T}$ changes the sign of time:

$$\mathcal{T} : t \to -t.$$

In terms of the position and momentum operators x and p,

$$\begin{aligned} \mathcal{P} : x \to -x,\ p \to -p \\ \mathcal{T} : x \to x,\ p \to -p \end{aligned} \tag{1}$$

$\mathcal{P}$ and $\mathcal{T}$ must preserve the canonical commutation relation $[x, p] = i\hbar$ - let's check that they do:

$$\begin{aligned} \mathcal{P}[x,p]\mathcal{P}^{-1} &= \mathcal{P}xp\mathcal{P}^{-1} - \mathcal{P}px\mathcal{P}^{-1} \\ &= \mathcal{P}x\mathcal{P}^{-1}\mathcal{P}p\mathcal{P}^{-1} - \mathcal{P}p\mathcal{P}^{-1}\mathcal{P}x\mathcal{P}^{-1} \\ &= (-x)(-p) - (-p)(-x) = [x,p] = i\hbar. \end{aligned}$$

Nothing new there... how about $\mathcal{T}$?

$$\begin{aligned} \mathcal{T}[x,p]\mathcal{T}^{-1} &= \mathcal{T}xp\mathcal{T}^{-1} - \mathcal{T}px\mathcal{T}^{-1} \\ &= \mathcal{T}x\mathcal{T}^{-1}\mathcal{T}p\mathcal{T}^{-1} - \mathcal{T}p\mathcal{T}^{-1}\mathcal{T}x\mathcal{T}^{-1} \\ &= (x)(-p) - (-p)(x) = [p,x] = -i\hbar \\ &= \mathcal{T}i\hbar\mathcal{T}^{-1}. \end{aligned}$$

While $\mathcal{P}$ is unitary, to preserve this commutation relation we must choose $\mathcal{T}$ to be *anti*-unitary, so that time reversal returns the complex conjugate of any number it acts upon, i.e. $\mathcal{T}i\mathcal{T}^{-1} \to -i$. Formally,

Definition 2.1. An operator A is *anti-unitary* if $\langle A\psi|A\phi\rangle = \langle\psi|\phi\rangle^* = \langle\phi|\psi\rangle$ for arbitrary states $|\psi\rangle$ and $|\phi\rangle$.

Remark. Anti-unitary operators are automatically *anti-linear*, i.e. $A(\lambda u + v) = \lambda^* u + \phi v$ for complex λ and vectors u and v. Likewise, unitary operators are automatically linear.

$\mathcal{P}$ and $\mathcal{T}$ are characterized by the following:

$$\begin{aligned} \mathcal{P}^2 = \mathcal{T}^2 = I, \\ [\mathcal{P}, \mathcal{T}] = 0. \end{aligned} \tag{2}$$

2.2 The Parity-Time Reversal Operator

$\mathcal{PT}$ symmetry seems natural when thought of in the context of special relativity, when space and time are brought together in a single four-vector:

$$\mathcal{PT}\colon (\vec{r}, t) \to (-\vec{r}, -t)$$

What do this operator's eigenvalues λ look like? Let $|\psi\rangle$ be an eigenstate of $\mathcal{PT}$. Then, using Eqns. 1 and 2, we can write

$$\mathcal{PTPT}\,|\psi\rangle = \mathcal{PT}\lambda\,|\psi\rangle \implies |\psi\rangle = \lambda^*\lambda\,|\psi\rangle \implies |\lambda|^2 = 1 \tag{3}$$

Thus the eigenvalues of the $\mathcal{PT}$ operator are of the form $\lambda = e^{i\theta}$ for some $\theta \in [0, 2\pi)$.

Definition 2.2. An operator A is $\mathcal{PT}$ *symmetric* if $[A, \mathcal{PT}] = 0$.

So, what can we say about a $\mathcal{PT}$ symmetric operator H at this point? Well, at the very least H and $\mathcal{PT}$ commute, so if H has eigenstate $|\psi\rangle$ and eigenvalue E, we have

$$\begin{aligned} H|\psi\rangle &= E|\psi\rangle \\ H(\mathcal{PT}|\psi\rangle) = \mathcal{PT}H|\psi\rangle &= \mathcal{PT}E|\psi\rangle = E^*(\mathcal{PT}|\psi\rangle) \end{aligned} \tag{4}$$

So E^* is also an eigenvalues of H, corresponding to the eigenstate $\mathcal{PT}|\psi\rangle$. Thus $\mathcal{PT}$ symmetry ensures that *all eigenvalues show up in complex-conjugate pairs.*

Definition 2.3. An operator H has *unbroken* $\mathcal{PT}$ *symmetry* if H and $\mathcal{PT}$ can be diagonalized by the same eigenstates. That is, if $|\psi\rangle$ is an eigenstate of H, then $A|\psi\rangle = E|\psi\rangle$ implies that $\exists\lambda$ such that $\mathcal{PT}|\psi\rangle = \lambda|\psi\rangle$.

Remark. In class we learned that Hermitian operators A and B are simultaneously diagonalizable if they commute, i.e. $[A, B] = 0$. Here, $\mathcal{PT}$ is not Hermitian, and the Hermiticity of H is not guaranteed.

Definition 2.4. We say that $\mathcal{PT}$ symmetry has been *spontaneously broken* when H and $\mathcal{PT}$ are no longer simultaneously diagonalizable. See Example 2.4.5.

Remark. An example of spontaneous symmetry breaking in another context: magnets will pick a direction to align with even when the Hamiltonian describing them is rotationally invariant!

We are now ready to prove our punchline:

Claim. Unbroken $\mathcal{PT}$ symmetry is sufficient for real energy spectra.

Proof. Let non-Hermitian operator H have unbroken $\mathcal{PT}$ symmetry. Then, H and $\mathcal{PT}$ can be simultaneously diagonalized by the eigenstate $|\psi\rangle$ of H:

$$\begin{aligned} H|\psi\rangle &= E|\psi\rangle \\ \mathcal{PT}|\psi\rangle &= \lambda|\psi\rangle = e^{i\theta}|\psi\rangle \end{aligned} \tag{5}$$

Operating $\mathcal{PT}$ on the first equation:

$$\mathcal{PT}H|\psi\rangle = \mathcal{PT}E|\psi\rangle = E^*\mathcal{PT}|\psi\rangle = E^*e^{i\theta}|\psi\rangle \tag{6}$$

Since H and $\mathcal{PT}$ commute, $\mathcal{PT}H|\psi\rangle = H\mathcal{PT}|\psi\rangle = E\mathcal{PT}|\psi\rangle = Ee^{i\theta}|\psi\rangle$.

Hence $E = E^*$, and the spectrum of H is real. □

2.3 Examples

Let's first take a look at some riffs on our favorite one-dimensional potential, the simple harmonic oscillator. In the subsequent examples, we follow the convention of [2] and set $\hbar = \omega = m = \frac{1}{2} = 1$.

Example 2.4.1. A warmup: the quintessential Hamiltonian for our beloved oscillator is $p^2 + x^2$, with positive definite energy eigenvalues $E_n = 2n + 1$.

Example 2.4.2. The combination ix is $\mathcal{PT}$ invariant, so adding it to our SHO Hamiltonian still returns a positive definite spectrum: $E_n = 2n + \frac{5}{4}$.

Example 2.4.3. The Hamiltonian $p^2 + ix^3 + ix$ has $\mathcal{PT}$ symmetry and has a positive definite spectrum.

Example 2.4.4. The Hamiltonian $p^2 + ix^3 + x$ does *not* have $\mathcal{PT}$ symmetry and has a wholly complex energy spectrum.

Example 2.4.5. The Bender-Boettcher potential that kickstarted all of this hullabaloo about $\mathcal{PT}$ symmetric non-Hermitian quantum mechanics is given by $H = p^2 - (ix)^N$ for $N \in \mathbb{R}$. A plot of the energy spectrum of this Hamiltonian is shown in Fig. 1. For $N \geq 2$, the spectrum is real and positive. For $1 < N < 2$, there are a finite number of real eigenvalues and an infinite number of complex-conjugate eigenvalue pairs. As $N \to 1^+$, the lowest energy eigenvalue diverges. There are *no* real eigenvalues for $N \leq 1$.

A phase transition occurs at the critical value $N_c = 2$, corresponding to the standard simple harmonic oscillator. $\mathcal{PT}$ symmetry is *spontaneously broken* at this point: approaching it from the right, we get a real energy eigenvalue; approaching it from the left, we get a complex one. Though the Hamiltonian itself remains $\mathcal{PT}$-invariant, its eigenvalues do not. To put it another way, the ground state of the system does not share the same symmetries as the Hamiltonian! Pretty cool, huh?

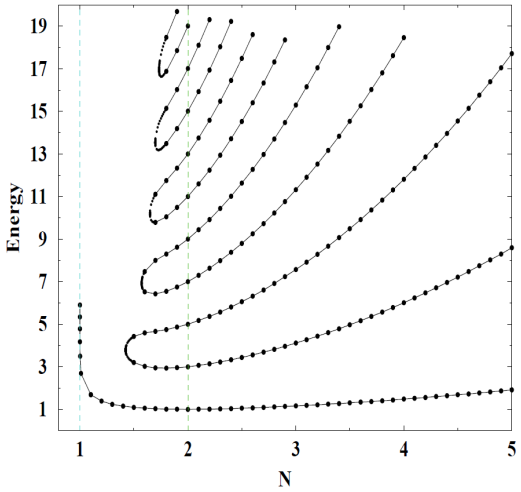


Figure 1: Energy levels for the Hamiltonian $H = p^2 - (ix)^N$. There is a phase transition at $N_c = 2$, corresponding to the simple harmonic oscillator Hamiltonian $p^2 + x^2$. Source: [2]

2.4 Pseudo-Hermiticity

As mentioned above, $\mathcal{PT}$ symmetry alone does *not* guarantee a real energy spectrum.

A different, necessary criteria for the spectrum of a non-Hermitian Hamiltonian to be purely real can be found using pseudo-Hermiticity ([13]). We give a cursory overview of this property here:

Definition 2.5. Let V be an inner product space. Then a linear operator $O: V \to V$ is η-*pseudo-Hermitian* if there exists a Hermitian linear automorphism η such that $O^\dagger = \eta O \eta^{-1}$.

Remark. Clearly, if $\eta = 1$ then we obtain the condition for Hermiticity. Pseudo-Hermiticity is thus a generalization of Hermiticity.

Example 2.5.1. Now, consider a $\mathcal{PT}$ symmetric Hamiltonian of the form $H = p^2 + V(x)$, where $V(x) = V_+(x) + iV_-(x)$ has even real component $V_+(x)$ and odd imaginary component $V_-(x)$. This condition that $V(x) = V^*(-x)$ is, in fact, necessary for a Hamiltonian to be $\mathcal{PT}$ symmetric (this follows from a straightforward application of Definition 2.2 to the one-dimensional Schrödinger equation). Then,

$$H^\dagger = p^2 + V_+(x) - iV_-(x) = p^2 + V_+(-x) + iV_-(-x) = \mathcal{P}H\mathcal{P} = \mathcal{P}H\mathcal{P}^{-1}.$$

H is therefore $\mathcal{P}$-psuedo-Hermitian.

Example 2.5.2. $H_1 = p^2 + x^2 p$ is $\mathcal{PT}$ symmetric but *not* $\mathcal{P}$-pseudo-Hermitian.

Example 2.5.3. $H_2 = p^2 + i(x^2 p + p x^2)$ is $\mathcal{P}$-pseudo-Hermitian but *not* $\mathcal{PT}$ symmetric.

We take the condensed version of the following theorem from the delightfully written [11], from which we have adapted much of our previous discussion of $\mathcal{PT}$ symmetry. But first, a useful definition:

Definition 2.6. Let H be a Hamiltonian with a complete *biorthonormal eigenbasis* $\{|\psi_n, a\rangle, |\phi_n, a\rangle\}$. Then H has the following properties:

- $H|\psi_n, a\rangle = E|\psi_n, a\rangle,\ H^\dagger|\phi_n, a\rangle = E^*|\phi_n, a\rangle$
- $\langle \phi_m, b|\psi_n, a\rangle = \delta_{mn}\delta_{ab}$
- $\sum_n \sum_{a=1}^{d_n} |\phi_n, a\rangle \langle \psi_n, a| = \sum_n \sum_{a=1}^{d_n} |\psi_n, a\rangle \langle \phi_n, a| = 1,$

where d_n is the multiplicity (degeneracy) of the eigenvalue E_n, and a, b are degeneracy labels.

Theorem. (Mostafazadeh (2002)) Let H be a Hamiltonian that acts in a Hilbert space, has a discrete spectrum, and admits a complete set of biorthonormal eigenvectors $\{|\psi_n\rangle, |\phi_n\rangle\}$. Then the spectrum of H is real if and only if there is an invertible linear operator O such that H is $OO^\dagger$-pseudo-Hermitian, i.e. $H = (OO^\dagger)H^\dagger(OO^\dagger)^{-1}$.

We will not go more in detail on pseudo-Hermitian operators here, but [13] has a lengthy discussion of more of their neat properties, if you're interested in reading more.



Figure 2: No, not this kind... Source: Google Images

3 Exceptional Points (EPs)

Consider a minimal example of a non-Hermitian, $\mathcal{PT}$ symmetric system ([11]), given by

$$H = \begin{pmatrix} i\gamma & \kappa \\ \kappa & -i\gamma \end{pmatrix} = \kappa\sigma_1 + i\gamma\sigma_3, \tag{7}$$

where $\gamma, \kappa \in \mathbb{R}$, $\gamma, \kappa \geq 0$, and we have used σ_j, $j = 1, 2, 3$ to denote the Pauli matrices

$$\sigma_1 = \begin{pmatrix} 0 & 1 \\ 1 & 0 \end{pmatrix}, \sigma_2 = \begin{pmatrix} 0 & -i \\ i & 0 \end{pmatrix}, \sigma_3 = \begin{pmatrix} 1 & 0 \\ 0 & -1 \end{pmatrix}. \tag{8}$$

H is $\mathcal{PT}$ symmetric under $\mathcal{P} = \sigma_1$ and $\mathcal{T}$ being the complex conjugation operator (Exercise: check it!).

Let's pause here for just a moment. Intuitively, $\mathcal{P}$ and $\mathcal{T}$ are some flavor of coordinate transforms that we can visualize pretty easily. But none of that exists in matrix space! Yet somehow we can write down matrix representations of systems and operators, and the math all still manages to check out with the abstracted Hilbert space properties we looked at in Section 2.2. If that smells fishy to you, check out this link, and let your mind at ease.

Getting back to our regularly scheduled program: the eigenvalues and eigenvectors of H are given by

$$E_\pm = \pm\sqrt{\kappa^2 - \gamma^2}, \; |\pm\rangle = \begin{pmatrix} i\gamma \pm \sqrt{\kappa^2 - \gamma^2} \\ \kappa \end{pmatrix} \tag{9}$$

There are a few observations we can make here:

Observation 1. These two eigenstates are *not* orthogonal:

$$\langle +|-\rangle = 2\gamma(\gamma + i\sqrt{\kappa^2 - \gamma^2}) \neq 0$$

unless H is trivial (which doesn't really count, because it's boring).

From the above example we see that $\mathcal{PT}$ symmetry does *not* guarantee orthogonal eigenstates! However, they still form a complete basis, with one exception that we will get to shortly.

There are three cases to consider:

Observation 2. For $\gamma \leq \kappa$, the spectrum of H is purely real.

Observation 3. For $\gamma > \kappa$, the spectrum of H is purely imaginary.

Observation 4. $\mathcal{PT}$ symmetry is *spontaneously broken* at $\gamma = \kappa$. As $\gamma \to \kappa$ from both sides, *both* pairs of eigenvalues (real and imaginary) coalesce to a single eigenvalue at $E = 0$, and the eigenvectors of H become parallel. At this point, the single eigenstate of H does *not* span.

Remark. Though the eigenstates of a $\mathcal{PT}$ symmetric operator may not form an orthonormal basis, we can in general *construct* an one from them. For instance, in the above example, we can use Gram-Schmidt for $\kappa \neq \gamma$, and can select any orthogonal vector for $\kappa = \gamma$.

These symmetry-breaking points in parameter space - of the form (γ, κ) in this case - have been dubbed *exceptional points* (EPs) by [10]. They are the boundaries between regions of *unbroken* $\mathcal{PT}$ symmetry, where a Hamiltonian H has all real eigenvalues, and regions of *broken* $\mathcal{PT}$ symmetry where H has at least one pair of complex conjugate eigenvalues. EPs are distinct from extended play records, which are also known as EPs (see Fig. 2).

We have thus far focused on EPs in the context of $\mathcal{PT}$ symmetric non-Hermitian systems, as branch point singularities demarcating the boundary between the real and complex eigenspectra. However, they are by no means exclusive to this regime! [7] has a lovely discussion of EPs in the more general context of non-Hermitian quantum mechanics by looking at two EPs stemming from a (not necessarily $\mathcal{PT}$ symmetric) Hamiltonian.

4 Applications

EPs give rise to exceptionally weird physical phenomena in mechanics, electromagnetism, atomic and molecular physics, quantum phase transitions, quantum chaos, and more ([7])! Full exploration of these applications is beyond the scope of this paper, but we can at least dip our toes into a field that has made considerable progress (both theoretical and experimental) on furthering our understanding of exceptional point physics and its more practical applications in the last few years, optics.

4.1 Optical Interpretation

Exceptional point physics lends itself well to understanding gain/loss systems, which are especially prevalent in optics and photonics, as optical modes (the analogues to energy eigenstates) in microcavities are subject to losses from absorption and radiation. Such open systems can often be well-described by non-Hermitian Hamiltonians. [17] provides a mathematically rigorous physical interpretation of interactions with $\mathcal{PT}$ symmetric local potentials as electromagnetic waves traveling through a planar waveguide filled with equal parts gain and absorbing media.

This realization spurred a flurry of experimental realizations of $\mathcal{PT}$ symmetric non-Hermitian systems, as experimentalists rapidly discovered that $\mathcal{PT}$ symmetry could be readily established in coupled resonators with spatially balanced gain (amplification of optical

power) and loss elements [9]. Their setups allowed for direct control over the energy exchange process via fine-tuning the coupling between the resonators [8].

To connect back with our toy model in Equation 7, we can think of γ ($-\gamma$) as the optical gain (loss) of one of two identical coupled optical elements, for instance waveguides or resonators. The gain and loss γ describes is the coupling of each element to the outside world, i.e. the rate of information going in/coming out from the external environment. Since γ is constant here, it describes a constant rate of external noise. Parity $\mathcal{P}$ interchanges the gain and loss elements, while time reversal $\mathcal{T}$ converts gain to loss and vice-versa ($\gamma \leftrightarrow -\gamma$). The strength of interaction of these two elements is given by their coupling constant κ, describing the rate of signal transfer between the two elements - more coupling (higher values of κ) means less loss of signal (photons).

When $\gamma \ll \kappa$, the coupling between the optical devices is much larger than their coupling to the outside world, and the system is $\mathcal{PT}$ symmetric. When $\gamma \gg \kappa$, the rate of white noise from the outside world dominates over the rate of information transfer between the gain and loss elements. As a result, a qualitatively different set of eigenstates emerges. In our example, these would be the states corresponding with the purely imaginary spectrum of the Hamiltonian given in equation 7, i.e. exponentially growing and decaying modes. $\gamma = \kappa$, as before, corresponds to an EP where some eigenmodes of the system coalesce. As mentioned previously, the eigenstates of the system no longer form a complete basis at this point, thus rendering some modes inaccessible.

As we saw, exceptional points naturally arise from parameter-dependent eigenvalue problems. Naturally, this connection between $\mathcal{PT}$ symmetric systems and finely tunable experimental parameters set off a flurry of experimental realizations of EP physics in optics, for instance, in achieving stable single-mode lasers [9][5], and demonstrating topological chirality [4].

This last feature merits mentioning, if only because it can be more-or-less understood in a visually appealing, not overly-technical way - see Fig. 3. The surfaces shown are Riemann surfaces, each comprised of two single-valued Riemann sheets (red and blue) corresponding to two transverse waveguide modes. See Appendix A for a cursory overview of Riemann surfaces, and a slightly more geometrical exploration of an exceptional point. Basically, the direction - clockwise or counter-clockwise - in which an EP is non-adiabatically (you couldn't even do it adiabatically if you tried! See [4]) encircled in parameter space determines the final eigenstate, *not* the state's initial position, as one might expect. Circling direction then effectively acts as an asymmetric mode switch between different waveguide modes, opening the door to applications in system control for light of varying wavelengths.

4.2 Sensors

Sensors are everywhere - motion sensors for automatic doors and faucets, infrared sensors in home security systems, image sensors in digital cameras, gas detection sensors to monitor carbon monoxide levels, the list goes on. And the smaller the sensor, the better: microsensors tend to make measurements faster and more accurately than their macroscopic counterparts [20]. It should thus come as no surprise that optical microcavities, known for their ability to enhance light–matter interactions in a very confined volume, are prime candidates for sensing applications [3].

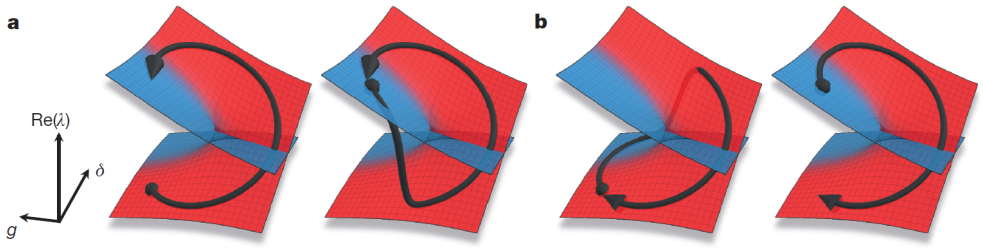


Figure 3: (a) Dynamics of two states starting on different Riemann sheets in $g-\delta$ (coupling and detuning, i.e. the difference between the system resonance frequency and the laser's optical frequency, respectively) space during a counter-clockwise loop around the EP (branch point, center); (b) Same as (a), but for a clockwise loop around the EP. Source: [4]

So what does this have to do with our previous discussion? A degeneracy of energy levels - and hence resonant frequencies - can be lifted by a small perturbation, leading to a detectable splitting between them. As such, such a degeneracy can serve as a basic element of a sensor [19].

What a coincidence - we now know of two such degeneracies! The first is the typical eigenvalue degeneracy, called a *diabolic point* (DP). DPs are characterized by degenerate eigenvalues with eigenstates that can always be chosen to be linearly independent. The second is, of course, an exceptional point. EPs are *fundamentally distinct* from DPs, and refer to the coalescence of both eigenvalues *and* their corresponding eigenstates. But whereas a perturbation of strength ϵ near a DP leads to an frequency splitting proportional to ϵ, the same magnitude perturbation near an EP results in a splitting that scales with $\epsilon^{1/2}$ [10]. This was experimentally demonstrated by [3], and others. See Fig. 4 for a schematic topological comparison between DPs and EPs. Thus, for sufficiently small perturbations, this eigenfrequency splitting enhancement can be exploited to improve the performance of microcavity sensors operating at EPs [19].

A single EP is commonly called a "second-order" exceptional point, in reference to the coalescence of two eigenstates. Note, then, that there are no such things as "first-order" EPs, which make neither physical nor logical sense (what would it mean for a single eigenvalue/eigenmode to be degenerate?). But if you can get a square-root splitting with a second-order EP, why not try for something even better with a third-order one?

We now focus our discussion on the work of [8], who used three coupled resonators (loss, gain, and neutral) to engineer a third-order $\mathcal{PT}$ symmetric photonic molecule supporting a third-order EP. Fig. 5 schematizes the setup of a coupled three micro-ring laser system used by [8] to observe a third-order EP. The setup is almost exactly the same as one we might use in a binary $\mathcal{PT}$ symmetric system with two resonators, as discussed in Section 4.1 - identical gain and loss cavities with coupling strength κ, but with an additional neutral resonator stuck in between.

Of course, for a third-order EP we expect *three* converging eigenvalues, so we must modify

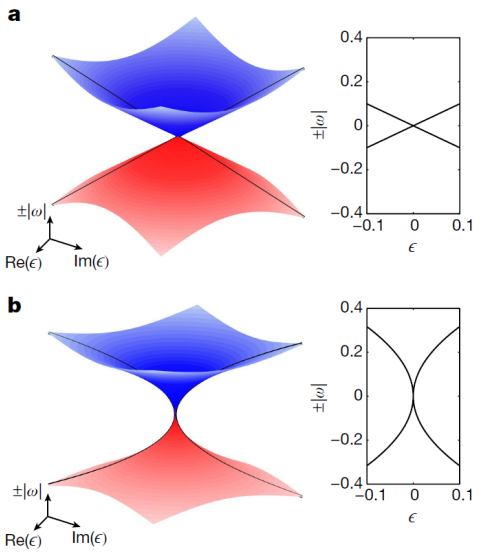


Figure 4: Topological surfaces characterizing the complex frequency ω of a) a typical diabolic point (DP; eigenvalue degeneracy) and b) an exceptional point (EP), as functions of (the magnitude of) small perturbations ϵ of an optical sensor. Frequency splittings are proportional to ϵ near a DP, and proportional to $\epsilon^{1/2}$ near an EP. Source: [3]

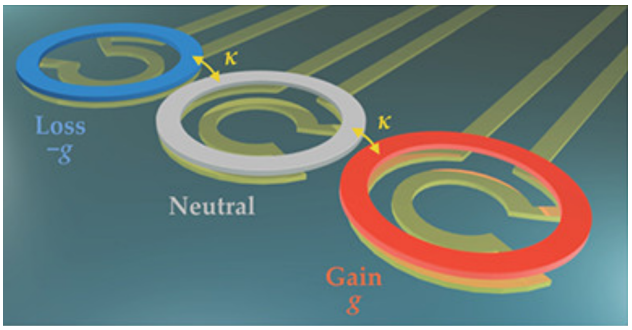
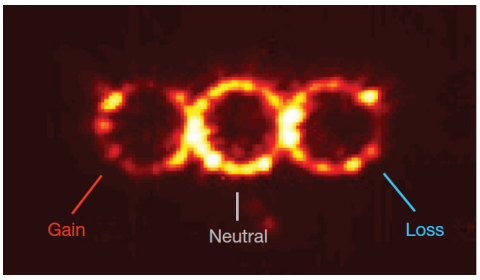
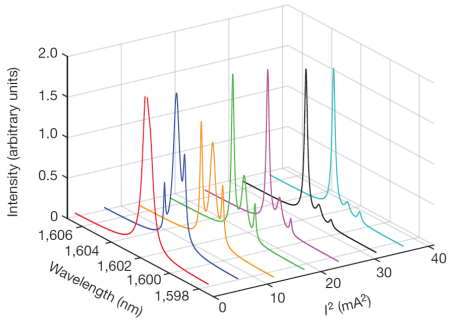


Figure 5: Setup of a $\mathcal{PT}$ symmetric ternary micro-ring laser system used to detect a third-order EP. Gain, loss, and neutral resonators are colored red, blue, and grey. Source: [12]



(a) Laser intensity profile in a system of three identical coupled resonators at a third-order exceptional point.



(b) The three eigenfrequencies split as the system moves away from the third-order EP when one of the micro-ring lasers (see Fig 5) is heated with a current I.

Figure 6: Experimental results of a ternary $\mathcal{PT}$ symmetric system at and around a third-order exceptional point. Source: [8]

the Hamiltonian in equation 7:

$$H = \begin{pmatrix} ig + \epsilon & \kappa & 0 \\ \kappa & 0 & \kappa \\ 0 & \kappa & -ig \end{pmatrix} \tag{10}$$

where g $(-g)$ stands for the gain (loss) of the identical resonators, κ is their coupling strength, and we have added a tiny perturbation ϵ to test the expected eigenvalue divergence of $\epsilon^{1/3}$. When the system is not perturbed, i.e. $\epsilon = 0$, its (complex) eigenfrequencies ω are given by the cubic equation

$$\omega(\omega^2 + g^2 - 2\kappa^2) = 0. \tag{11}$$

From equation 11, the eigenfrequencies all coalesce at $\omega = 0$ when the gain/loss $g = \kappa\sqrt{2}$. At $\omega = 0$, the system exhibits a third-order EP, and all eigenvectors coalesce at the (normalized) state $(-1, i\sqrt{2}, 1)/4$. This which tells us that the energy in the central (neutral) cavity is twice that of the neighboring cavities experiencing gain and loss. Figure 6a shows the measured intensity profile of the coupled ternary system, as captured by a charge-coupled device (CCD). Image analysis reveals a distribution of (1, 1.95, 1.16), where the neutral cavity indeed stores nearly double the energy of its neighbors [8], as expected. Figure 6b shows how the eigenfrequencies split up as the applied perturbation ϵ increases, and the system moves away from the exceptional point at $\omega = 0$.

References

[1] Bender, Carl M. "PT symmetry in quantum physics: From a mathematical curiosity to optical experiments". In: *Europhysics News* 47.2 (2016), pp. 17–20. DOI: 10.1051/epn/2016201. URL: https://doi.org/10.1051/epn/2016201.

[2] Carl M. Bender and Stefan Boettcher. "Real Spectra in Non-Hermitian Hamiltonians Having $\mathcal{PT}$ Symmetry". In: *Phys. Rev. Lett.* 80 (24 June 1998), pp. 5243–5246. DOI: 10.1103/PhysRevLett.80.5243. URL: https://link.aps.org/doi/10.1103/PhysRevLett.80.5243.

[3] W. Chen et al. "Exceptional points enhance sensing in an optical microcavity". In: *Nature* 548 (Aug. 2017), pp. 192–196. DOI: 10.1038/nature23281. URL: https://doi.org/10.1038/nature23281.

[4] J. Doppler et al. "Dynamically encircling an exceptional point for asymmetric mode switching". In: *Nature* 537 (Sept. 2016), pp. 76–79. DOI: 10.1038/nature18605. URL: https://doi.org/10.1038/nature18605.

[5] Liang Feng et al. "Single-mode laser by parity-time symmetry breaking". In: *Science* 346.6212 (2014), pp. 972–975. ISSN: 0036-8075. DOI: 10.1126/science.1258479. URL: https://science.sciencemag.org/content/346/6212/972.

[6] Naomichi Hatano and David R. Nelson. "Localization Transitions in Non-Hermitian Quantum Mechanics". In: *Phys. Rev. Lett.* 77 (3 July 1996), pp. 570–573. DOI: 10.1103/PhysRevLett.77.570. URL: https://link.aps.org/doi/10.1103/PhysRevLett.77.570.

[7] W D Heiss. "The physics of exceptional points". In: *Journal of Physics A: Mathematical and Theoretical* 45.44 (Oct. 2012), p. 444016. ISSN: 1751-8121. DOI: 10.1088/1751-8113/45/44/444016. URL: http://dx.doi.org/10.1088/1751-8113/45/44/444016.

[8] H. Hodaei et al. "Enhanced sensitivity at higher-order exceptional points". In: *Nature* 548 (Aug. 2017), pp. 187–191. DOI: 10.1038/nature23280. URL: https://doi.org/10.1038/nature23280.

[9] Hossein Hodaei et al. "Parity-time–symmetric microring lasers". In: *Science* 346.6212 (2014), pp. 975–978. ISSN: 0036-8075. DOI: 10.1126/science.1258480. eprint: https://science.sciencemag.org/content/346/6212/975.full.pdf. URL: https://science.sciencemag.org/content/346/6212/975.

[10] Tosio Kato. *Perturbation theory for linear operators*. Berlin: Springer-Verlag, 1966.

[11] Vladimir V. Konotop, Jianke Yang, and Dmitry A. Zezyulin. "Nonlinear waves in $\mathcal{PT}$-symmetric systems". In: *Rev. Mod. Phys.* 88 (3 July 2016), p. 035002. DOI: 10.1103/RevModPhys.88.035002. URL: https://link.aps.org/doi/10.1103/RevModPhys.88.035002.

[12] J. L. Miller. "Exceptional points make for exceptional sensors". In: *Physics Today* 70.10 (2017), p. 23. DOI: 10.1063/PT.3.3717.

[13] Ali Mostafazadeh. "Pseudo-Hermiticity versus PT symmetry: The necessary condition for the reality of the spectrum of a non-Hermitian Hamiltonian". In: *Journal of Mathematical Physics* 43.1 (Jan. 2002), pp. 205–214. ISSN: 1089-7658. DOI: 10.1063/1.1418246. URL: http://dx.doi.org/10.1063/1.1418246.

[14] David R. Nelson and Nadav M. Shnerb. "Non-Hermitian localization and population biology". In: *Phys. Rev. E* 58 (2 Aug. 1998), pp. 1383–1403. DOI: 10.1103/PhysRevE.58.1383. URL: https://link.aps.org/doi/10.1103/PhysRevE.58.1383.

[15] Tommy Ohlsson. "Non-Hermitian neutrino oscillations in matter with PT symmetric Hamiltonians". In: *EPL (Europhysics Letters)* 113.6 (Mar. 2016), p. 61001. ISSN: 1286-4854. DOI: 10.1209/0295-5075/113/61001. URL: http://dx.doi.org/10.1209/0295-5075/113/61001.

[16] H. Qin et al. "Kelvin-Helmholtz instability is the result of parity-time symmetry breaking". In: *Physics of Plasmas* 26.3 (2019), p. 032102. DOI: 10.1063/1.5088498. eprint: https://doi.org/10.1063/1.5088498. URL: https://doi.org/10.1063/1.5088498.

[17] A Ruschhaupt, F Delgado, and J G Muga. "Physical realization of -symmetric potential scattering in a planar slab waveguide". In: *Journal of Physics A: Mathematical and General* 38.9 (Feb. 2005), pp. L171–L176. DOI: 10.1088/0305-4470/38/9/l03. URL: https://doi.org/10.1088%2F0305-4470%2F38%2F9%2Fl03.

[18] Teleman, C. *Riemann Surfaces*. https://math.berkeley.edu/~teleman/math/Riemann.pdf. Accessed: 2020-03-08. 2003.

[19] Jan Wiersig. "Enhancing the Sensitivity of Frequency and Energy Splitting Detection by Using Exceptional Points: Application to Microcavity Sensors for Single-Particle Detection". In: *Phys. Rev. Lett.* 112 (20 May 2014), p. 203901. DOI: 10.1103/PhysRevLett.112.203901. URL: https://link.aps.org/doi/10.1103/PhysRevLett.112.203901.

[20] J. Yan. *Machinery Prognostics and Prognosis Oriented Maintenance Management*. Wiley, 2014. ISBN: 9781118638767. URL: https://books.google.com/books?id=PraTBQAAQBAJ.

A Riemann Surfaces

Definition A.1. A function $f: X \to Y$ between two topological spaces X and Y is a *homeomorphism* if:

- f is a bijection
- f is continuous
- The inverse function f^{-1} is continuous

If such a function exists, X and Y are *homeomorphic*.

Remark. *Homeo*morphisms are distinct from *homo*morphisms, and in fact are bijective homomorphisms (isomorphisms) between topological spaces!

Example A.1.1. The classic example is that a donut (a torus) and a coffee mug are homeomorphic - there is a cute GIF of this on Wikipedia.

Example A.1.2. The graph of a differentiable function is homeomorphic to the domain of the function.

Disclaimer. Much of the following explanation comes courtesy of [18].

Consider the complex root function $w(z) = \sqrt{z}$. We can use polar coordinates to write $z = re^{i\theta} \implies w = \sqrt{r}e^{i\theta/2}$, $-\pi < \theta \leq \pi$.

Note that $w = w(z)$ is a multi-valued function: say we start at $z_0 = -r_0$, so $w(z_0) = \sqrt{-r_0} = i\sqrt{r_0}$. Travelling one full circle counter-clockwise, we end at $w = \sqrt{r_0}e^{(i\pi+2\pi)/2} = -i\sqrt{r_0}$, the opposite of where we began! We would need to circle around the origin a second time in order to get back to $w = i\sqrt{r_0}$. Note that this difference only appears for imaginary values of z.

Clearly something strange is happening - the function $w(z)$ is not itself discontinuous; rather, there is some ambiguity in the choice of value along the negative real axis. We can imagine taking a handy dandy pair of math scissors and making a *branch cut* along this axis, thus cutting out all the unsavory multi-valued bits of our function. Mathematically, we do this by redefining $w(z)$ as

$$w: \mathbb{C} \to \mathbb{C} \setminus \{\mathrm{Re}(\sqrt{z}) < 0 \vee (\mathrm{Re}(\sqrt{z}) = 0 \wedge \mathrm{Im}(\sqrt{z}) < 0)\},\ w(z) = \sqrt{z}. \tag{12}$$

We can also think of w as being composed of two distinct complex (z) planes, that give values of $\sqrt{z}$ differing by a sign (see Fig. 7). The graph of these two z-planes is a closed subset in $\mathbb{C}^2$:

$$S = \{\, (z, w) \in \mathbb{C}^2 \mid w^2 = z \,\},$$

but we can define a map that takes these 2-D coordinates to a *single* w-plane:

$$f: S \to \mathbb{C},\ f(z) = w. \tag{13}$$

That is, we can replace the complex plane with the graph of the function (in this case, its projection onto the w-axis) to obtain a single-valued function! Here, f is a homeomorphism of the graph S to its projection on the w-plane.

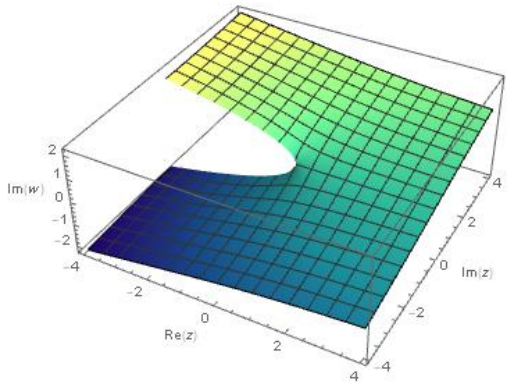


Figure 7: Discontinuity of the complex root function $w(z) = \sqrt{z}$. We can think of this function as being comprised of two distinct complex planes, separated by the real axis.

We call S a *Riemann surface* (see Fig. 8), in general a one-dimensional complex manifold composed of (up to infinitely many) *Riemann sheets*. In this example, S is comprised of two Riemann sheets, the two z-planes. Note that above the branch cut (the line where the surface intersects itself), the square root is single-valued. As we pass below the cut into the other branch of the function, we get $-\sqrt{z}$, also single-valued. Riemann surfaces help us to visualize multi-valued functions, such as $w(z) = \sqrt{z}$, as single-valued functions.

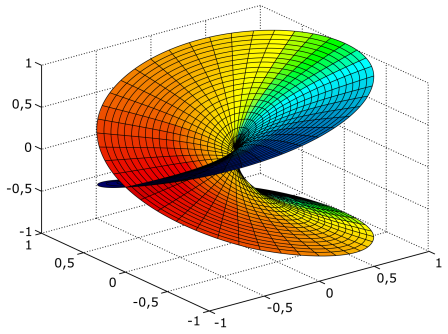


Figure 8: The Riemann surface for $\sqrt{z}$, comprised of two single-valued Riemann sheets ($+\sqrt{z}$ above the branch cut, and $-\sqrt{z}$ below). Horizontal axes represent the real and imaginary parts of z, and the vertical axis is the real part of $\sqrt{z}$. Source: Wikipedia